

Article

Analyzing the Mechanism of Drilling Losses in the Zhengning Oilfield in the Ordos Basin

Tuan Gu ¹, Shugang Yang ¹, Yunfeng Xiao ¹, Linpeng Zhang ¹, Fangquan Peng ², Xu Su ^{2,*}, Tao Fan ¹, Haiyang Wang ² and Desheng Zhou ²

¹ Exploration and Development Research Institute of Liaohe Oilfield Company, PetroChina, Panjin 124010, China; gutuan@petrochina.com.cn (T.G.); 13679161464@163.com (S.Y.); xiaoyunf@petrochina.com.cn (Y.X.); zlp0303@petrochina.com.cn (L.Z.); fantao414@163.com (T.F.)

² School of Petroleum Engineering, Xi'an Shiyou University, Xi'an 710065, China; 23212010116@stumail.xsyu.edu.cn (F.P.); wanghaiyang@xsyu.edu.cn (H.W.); dzhou@xsyu.edu.cn (D.Z.)

* Correspondence: 24111010032@stumail.xsyu.edu.cn

Abstract: Frequent wellbore loss incidents in the Mesozoic reservoirs of the Zhengning oilfield in the Ordos Basin, China, have severely impacted the development of tight oil and gas reservoirs in the basin. This study analyzed the mineral composition, microstructure, natural fracture distribution, and hydration–dispersion characteristics of rocks in the loss-prone intervals of the Mesozoic reservoirs using a laboratory experimental system. The effects of natural fractures and drilling fluid immersion on the mechanical properties and failure behavior of the rocks were investigated, and the wellbore loss mechanisms in the Mesozoic reservoirs of the Zhengning oilfield were comprehensively analyzed. Experimental results show that the reservoir rocks in the loss-prone intervals are widely distributed, with natural fractures having a width of 0.2–0.3 mm, and the clay mineral content is generally above 40%. When the relative content of illite/smectite interstratification exceeds 80%, the rock exhibits strong hydration–dispersion behavior, with a thermal recovery rate of less than 85%. Drilling fluid immersion causes the rock mass to become unstable. The presence of natural fractures and the hydration–dispersion effect significantly weaken the strength of the surrounding rock mass, leading to enhanced rock plasticity. During drilling, the expansion and interconnection of natural fractures, combined with the hydration–dispersion effect, are the main causes of wellbore loss incidents. Our study clarifies the mechanisms underlying wellbore loss incidents in the Zhengning oilfield and provides reliable experimental evidence for preventing such incidents in this area.

Keywords: Ordos Basin; drilling; rock mineral composition; rock mechanics



Academic Editors: Guanzheng Zhuang, Qiang Li and Manuel Pozo Rodríguez

Received: 23 December 2024

Revised: 13 January 2025

Accepted: 16 January 2025

Published: 17 January 2025

Citation: Gu, T.; Yang, S.; Xiao, Y.; Zhang, L.; Peng, F.; Su, X.; Fan, T.; Wang, H.; Zhou, D. Analyzing the Mechanism of Drilling Losses in the Zhengning Oilfield in the Ordos Basin. *Minerals* **2025**, *15*, 85. <https://doi.org/10.3390/min15010085>

Copyright: © 2025 by the authors. Licensee MDPI, Basel, Switzerland. This article is an open access article distributed under the terms and conditions of the Creative Commons Attribution (CC BY) license (<https://creativecommons.org/licenses/by/4.0/>).

1. Introduction

In the Ordos Basin, China's Zhengning oilfield is a key area rich in tight oil and gas resources, so it is crucial to China National Petroleum Corporation (CNPC)'s development strategy [1–3]. The region holds substantial potential, with estimates indicating large reserves vital for national energy security. However, drilling efficiency is hindered by recurrent lost circulation incidents, which increase operational costs and disrupt drilling timelines, challenging timely resource development [4,5]. Lost circulation impacts wellbore stability, formation integrity, and drilling safety [6–8]. Understanding its mechanisms is essential to identify contributing factors and develop effective mitigation strategies [9,10]. This knowledge is critical for optimizing drilling performance, ensuring safety, and sup-

porting sustainable operations in the Zhengning oilfield. Thus, addressing drilling losses is a priority to enhance resource extraction efficiency and reliability in this key region.

Current research on drilling loss mechanisms is analyzed through two primary approaches: numerical simulations and experimental studies. Numerical simulations have significantly advanced, enabling researchers to model the complex behavior of drilling fluids under various geological conditions [11–13]. These simulations primarily focus on stress variations around the wellbore, highlighting how increased pore pressure and stress concentrations can lead to fracture propagation. Fractures may form due to the interaction between the drilling fluid and the rock, leading to significant fluid loss, especially in formations with pre-existing weaknesses [14–17]. Experimental research complements these numerical findings by examining the physical properties of rocks and drilling fluids under controlled conditions [18–20]. Studies have shown that the hydration and dispersion of certain rock types can cause wellbore instability, weakening the rock and potentially leading to collapse [21,22]. For example, clays tend to expand when exposed to water-based drilling fluids, increasing permeability and fluid loss. Experimental setups also allow for the investigation of additional factors, such as temperature variations, fluid viscosity, and the effects of different additives in drilling mud. These factors can either mitigate or exacerbate lost circulation [23–25]. Recent advancements have introduced hybrid approaches that combine numerical and experimental methods, offering a more comprehensive understanding of lost circulation phenomena [26,27]. Research has also emphasized the importance of geological factors, such as natural fractures, faults, and the anisotropic nature of rock materials, which complicate the prediction and management of drilling losses [28–30]. Additionally, the influence of drilling parameters, such as weight on bit, rotation speed, and fluid properties, has been extensively studied to develop best practices for minimizing lost circulation incidents. Overall, this multifaceted approach highlights the need for a deep understanding of the mechanisms behind drilling losses, which is crucial for improving drilling efficiency and safety in challenging environments.

Research has also been conducted on efficient drilling for unconventional oil and gas reservoirs in the Ordos Basin, China. Wu et al. [31] proposed a digital DPM method that can monitor the relative variation of rock mechanical strength along the depth direction of a drill bit in real time. Liu et al. [32] studied the optimal trajectory design for horizontal wells in fractured tight sandstone reservoirs of the Ordos Basin. Zhang et al. [33] developed a novel drilling fluid system with enhanced plugging for carbonate reservoirs in the Ordos Basin. Zhang et al. [34] analyzed the mechanism of formation damage caused by wellbore losses and optimized the drilling fluid system based on their findings. Although some research achievements have been made in efficient drilling in the Ordos Basin, the drilling loss mechanisms and influencing factors in the Zhengning oilfield block of the Ordos Basin remain unclear.

To address the frequent lost circulation issues in the tight oil and gas reservoirs of the Zhengning oilfield, this study first analyzed the mineral composition, natural fracture distribution, and micro-pore throat characteristics of its lost circulation intervals using core samples. Based on this analysis, the hydration and dispersion properties of the reservoir rocks in these intervals were investigated. Finally, utilizing standard cores from the same lost circulation intervals, we examined the mechanical properties of the surrounding rock under various conditions. This research elucidates the mechanisms of lost circulation during drilling in the Zhengning oilfield, providing valuable theoretical guidance for the safe and efficient exploitation of tight oil and gas reservoirs in the Ordos Basin of China.

2. Analysis of Rock Characteristics in Loss Zones

Based on the characteristics of the drilling loss incident at the Zhengning oilfield, we conducted a study and analysis of the drilling loss mechanism in the area following the steps and sequence outlined in Table 1.

Table 1. The steps involved in the drilling loss analysis and their sequence.

Steps for Analyzing Drilling Losses	Experiment Type	Experimental Purpose
Rock characteristic analysis	(1) Steady-state displacement experiment (2) XRD diffraction analysis (3) Scanning electron microscopy (SEM) experiment	Analyze the permeability, porosity, mineral composition, and distribution size of natural fractures in the rock.
Hydration–dispersion characteristic analysis	(1) Rock water absorption experiment (2) Thermal recovery experiment	Analyze the water absorption capacity of different types of rocks and study the structural changes in the rock mass after water absorption.
Rock mechanical characteristic analysis	Triaxial compression experiment	Analyze the mechanical properties of rocks and study the impact of natural fractures and drilling fluid immersion on the mechanical performance of the rock.

Understanding the basic characteristics of reservoir rocks is fundamental for analyzing how losses occur during the drilling process. In the Ordos Basin's Zhengning oilfield, significant loss incidents frequently arise during drilling. To investigate the causes and mechanisms of drilling losses, we conducted core sampling (as shown in Figure 1) to analyze the rock characteristics of loss zones at different depths. Standard cylindrical rock samples with a length of 5.0 cm and a diameter of 2.5 cm were prepared using a wire-cutting machine. We tested the water displacement permeability and porosity of the cores from the loss zones using a steady-state displacement experimental setup, with the results summarized in Table 2. The experimental procedure was as follows: (1) Place the standard cylindrical rock sample in the lithology holder. (2) Turn on the displacement pump and inject distilled water into the rock pores at a constant pressure. (3) Once the flow rate at the outlet stabilizes, record the pressure at both ends of the holder and the flow rate at the outlet. (4) Calculate the porosity and water displacement permeability based on Darcy's law and the mass change of the core before and after displacement. As shown in Table 2, the rocks in the loss zones exhibit low porosity and permeability, with an average porosity of 3.89% and an average permeability of 0.044 mD. This indicates that, during drilling, the drilling fluid has difficulty flowing into the rock pores of the loss zones, which affects the pore pressure and effective stress field surrounding the wellbore.

Using XRD technology, we analyzed the main mineral content of rocks in the loss zones, with the results shown in Figure 2. The experimental procedure was as follows: (1) Select representative core samples and grind them into rock powder using a grinding machine. (2) Analyze the mineral composition of the samples using X-ray diffraction (XRD) equipment. The data indicate that the clay mineral content in the reservoir rocks of the loss zones is generally high, with the clay mineral content consistently exceeding 40% at different depths and reaching up to 70%. Quartz is the second most abundant mineral, averaging around 30%. The contents of potassium feldspar and plagioclase are quite low, collectively accounting for less than 10%. When clay mineral content is high, minerals such as montmorillonite and illite, which are prone to hydration and dispersion, may affect the mechanical properties of the rock under the invasion of drilling fluids.

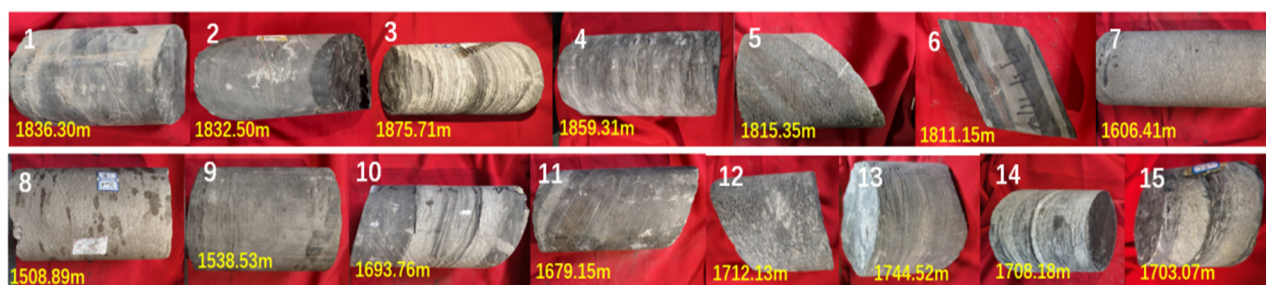


Figure 1. Core sampling during drilling at the Zhengning oilfield.

Table 2. Fundamental physical properties of major loss zone rocks.

Core Number	Porosity/%	Permeability/mD	Depth of Drilling Leakage Zone/m
1	4.76	0.090	1832.5
2	5.10	0.120	1836.3
3	3.83	0.030	1859.31
4	1.98	0.009	1875.71
5	5.35	0.064	1811.15
6	3.69	0.040	1815.35
7	3.22	0.050	1508.89
8	5.76	0.035	1538.53
9	3.35	0.040	1606.41
10	4.15	0.031	1679.15
11	2.36	0.020	1693.76
12	5.18	0.071	1712.13
13	3.31	0.026	1744.52
14	3.96	0.030	1703.07
15	2.34	0.010	1708.18

Based on this, we conducted further analysis of the clay mineral composition in the loss zone rocks, with the results displayed in Figure 3. The data reveal that the content of illite/montmorillonite interlayers in the clay minerals is generally high, averaging over 38%, with some samples approaching 90%. Illite is the second most abundant mineral component in the clay minerals, averaging around 30%. The contents of kaolinite and chlorite are relatively low. The illite/montmorillonite interlayer represents a transitional layer between the layered structures of illite and montmorillonite, exhibiting mixed characteristics in chemical composition and crystal structure. Given that montmorillonite is prone to hydration and dispersion, a high content of illite/montmorillonite interlayers suggests that the clay minerals in the loss zones may possess a certain degree of hydration and dispersion capability.

During drilling, natural fractures in the rock can become the primary channels for drilling fluid loss. Under the pressure of the fluid column in the wellbore, these natural fractures may further propagate, exacerbating the loss of drilling fluid. As shown in Figure 4, during the preparation of standard rock samples, we observed that the rocks in the loss zones contain natural fractures of varying sizes. The natural fractures in the reservoir of the loss zones are predominantly longitudinal. Using a vernier caliper, we measured the widths of the macro natural fractures present in the loss zone reservoir rocks, and the statistical results are presented in Figure 5. The data indicate that the width of the natural fractures has a wide distribution range, with the majority falling within the 0.2 mm to 0.3 mm range, accounting for over 30%. Natural fractures wider than 0.5 mm comprise as much as 14% of the total. During drilling, macro natural fractures with widths greater than 0.1 mm in the reservoir of the loss zones can easily begin to propagate under the static fluid column pressure in the wellbore, leading to drilling fluid loss. Once the

fractures begin to propagate, both their width and length can increase rapidly, resulting in larger-scale drilling fluid loss incidents.

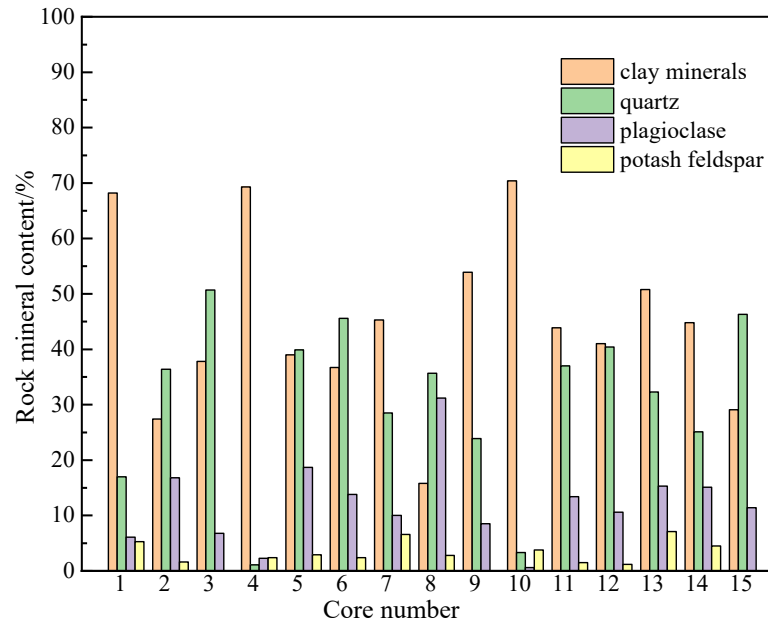


Figure 2. Analysis of main mineral content in reservoir rocks of loss zones.

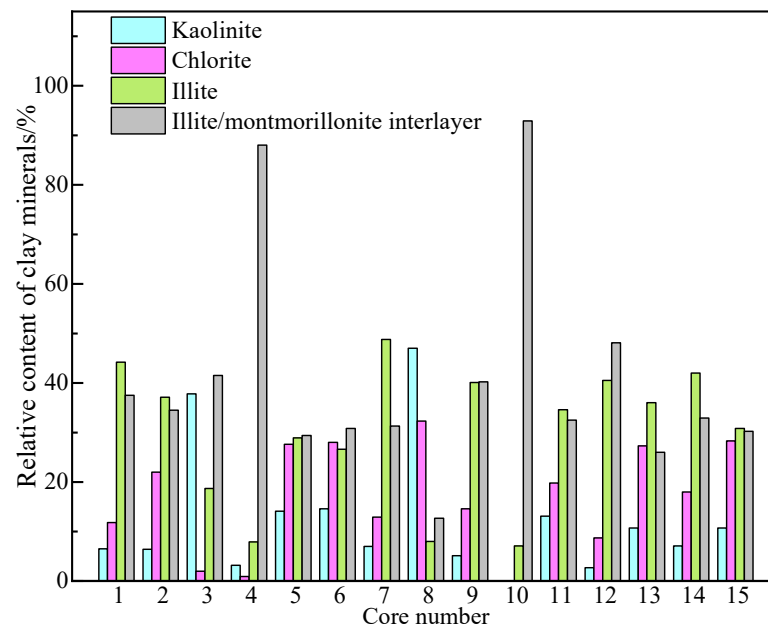


Figure 3. Analysis of relative content of clay minerals in loss zone rocks.

Additionally, we utilized scanning electron microscopy (SEM) to analyze the micro-pore structure of the rocks in the loss zones, with the results shown in Figure 6. The experimental procedure was as follows: (1) Select drilling core samples from different loss zones. (2) Use a cutting machine to cut the rock into samples of 0.5 cm × 0.5 cm. (3) Clean the surface of the samples and coat them with a thin layer of metal to enhance their conductivity. (4) Use scanning electron microscopy (SEM) to observe the microstructure of the rock surface and the morphology of natural fractures, and then measure the fracture width of the natural fractures. The data indicate that micro fractures in the loss zone rocks are also well developed. The fibrous clay minerals exhibit a flaky structure with a certain degree of orientation, interspersed with quartz crystals. Feldspar particles and fibrous clay

mineral particles contain micro fractures of varying widths. We conducted a statistical analysis of the widths of the micro natural fractures in the loss zone rocks, with the results presented in Figure 7. The analysis reveals that the widths of the micro natural fractures primarily range from 0.5 μm to 2 μm , accounting for over 60%, while those exceeding 3.0 μm are relatively rare. During drilling, once the drilling fluid invades the rock pores, it may cause the micro natural fractures to continue to propagate, forming larger fractures. The continued propagation of micro natural fractures during drilling fluid loss not only reduces the strength of the rock surrounding the wellbore but may also connect with larger fractures, resulting in more significant fluid loss. Thus, in the context of the Zhengning oilfield in the Ordos Basin, it is essential to incorporate sealants that can block micro fractures during drilling to prevent the propagation of micro fractures into larger ones. Overall, the analyses in Figures 4–7 suggest that the presence of large macro natural fractures and micro natural fractures in the loss zone rocks is one of the causes of drilling fluid loss incidents. During drilling, large natural fractures directly provide pathways for fluid loss, and under the pressure of the fluid column in the wellbore, these macro natural fractures may continue to propagate and connect with micro natural fractures, resulting in even larger fluid loss.

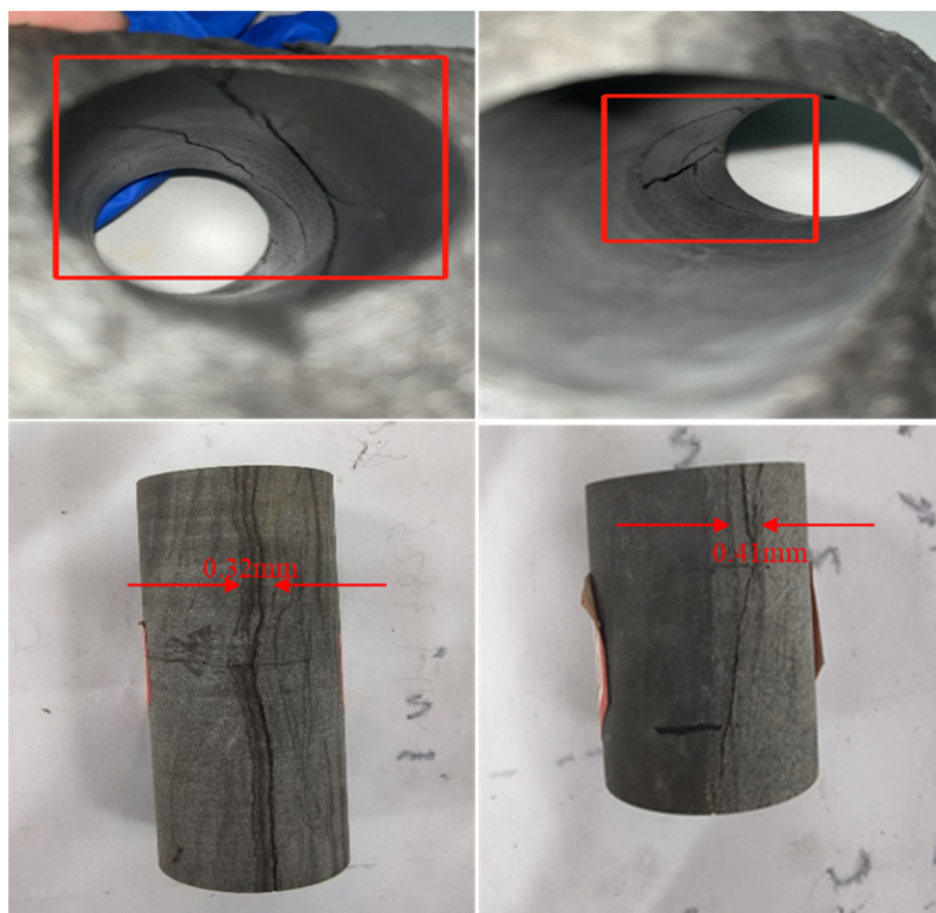


Figure 4. Distribution of macro natural fractures in reservoir rocks of loss zones.

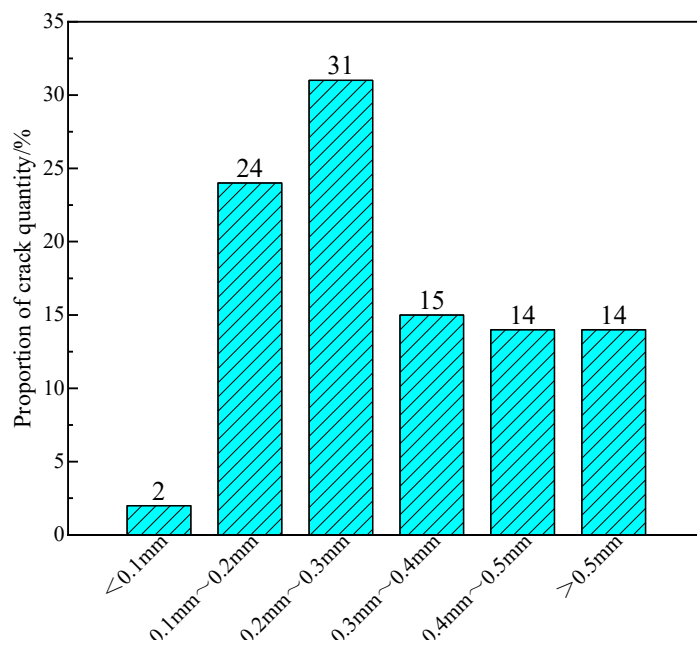


Figure 5. Statistical results of macro natural fracture widths in loss zone rocks.

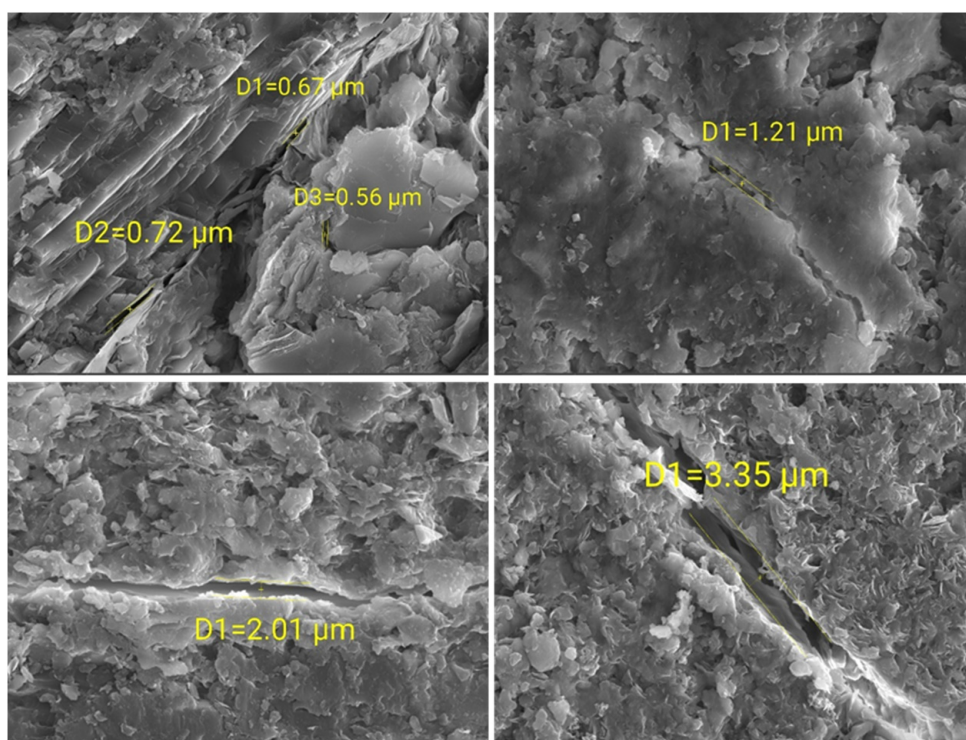


Figure 6. Microstructural features and distribution of micro natural fractures in reservoir rocks of loss zones.

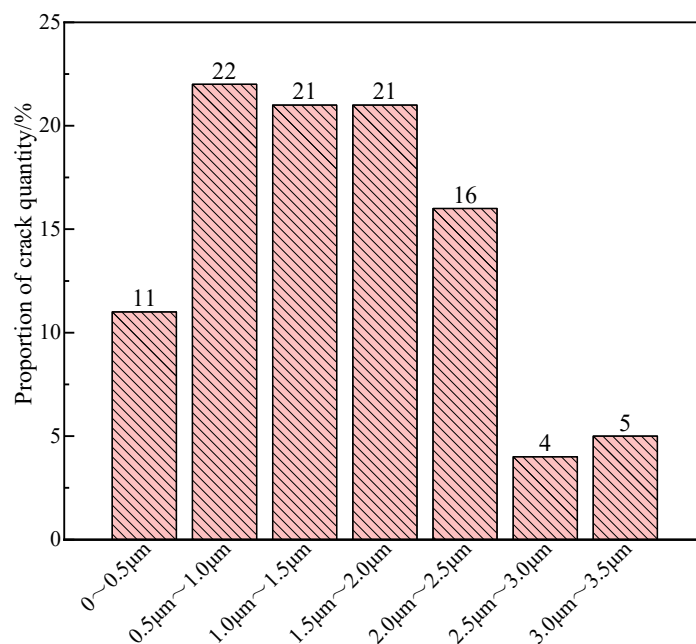


Figure 7. Statistical results of micro natural fracture widths in reservoir rocks of loss zones.

3. Analysis of Hydration and Dispersion Characteristics of Rocks in Loss Zones

In the previous section, we analyzed the mineral composition of rocks in the loss zones, confirming that illite/montmorillonite interlayers are a primary component of clay minerals, which may induce hydration and dispersion in the rocks, affecting their mechanical properties. For this section, we first conducted water absorption experiments to analyze the short-term water absorption performance of four rock samples (core numbers 3, 4, 10, and 12) with a high clay mineral content. The experimental procedure was as follows: (1) Dry the prepared rock samples, record their mass, and measure their volume. (2) Suspend the cores in distilled water and monitor the mass changes during the absorption process. (3) After 48 h of soaking, remove the cores and measure their volume. Figure 8 presents the mass change curve over time for the rock samples immersed in distilled water. Figure 8 shows the curve of mass change over time for the rock samples immersed in distilled water. The results indicate that when the relative content of illite/montmorillonite interlayers in the clay minerals is below 50% (cores 3 and 12), the water absorption curve is relatively flat and the overall absorption is low. Conversely, when the relative content exceeds 80% (cores 4 and 10), the rocks exhibit rapid water absorption, with a significantly larger total absorption amount.

Figure 9 illustrates the hydration and dispersion behavior of the rock samples numbered 3, 4, 10, and 12 after long-term immersion in distilled water. The experimental procedure was as follows: (1) Select drilling core samples with identical quality and intact rock structure. (2) Soak the selected drilling core samples in a container filled with distilled water, ensuring that the entire rock sample is submerged. (3) Observe the changes in the rock structure as the core samples are soaked in distilled water for different durations. As shown in Figure 9, rocks with a low content of illite/montmorillonite interlayers (cores 3 and 12) exhibited no significant structural changes even after being immersed for 20 days, indicating weak hydration and dispersion capabilities. In contrast, the rocks with a high content of illite/montmorillonite interlayers (cores 4 and 10) began to show structural changes after 10 days of soaking, with noticeable chipping and flaking occurring. As the soaking time increased, the hydration and dispersion effects intensified, leading to significant alterations in the rock structure and resulting in instability. We further compared the main and

side views of rock sample 10, which had the highest content of illite/montmorillonite interlayers, before and after soaking, as shown in Figure 10. Before immersion, core 10 displayed distinct horizontal bedding fractures with narrow widths. However, after immersion in distilled water, the rock structure underwent significant changes, with a marked increase in the width of the horizontal bedding fractures. Additionally, due to the hydration and dispersion effects, prominent vertical fractures formed. The interconnected fractures led to the chipping of the rock, rendering the structure unstable.

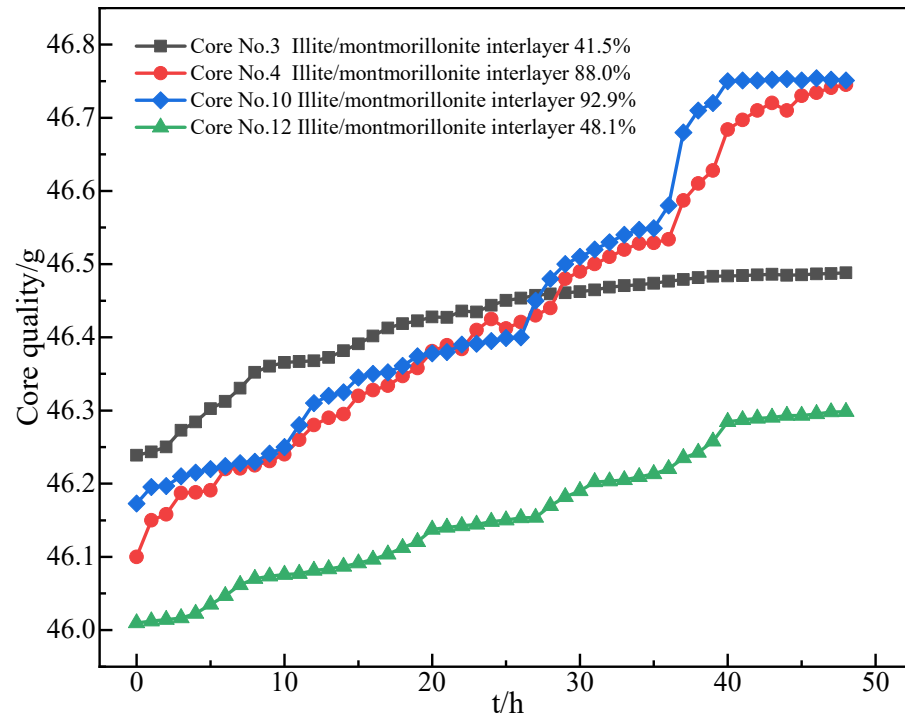


Figure 8. Results of water absorption experiments on rocks in loss zones.

Using thermal rolling recovery experiments, we further analyzed the thermal rolling recovery rates of these four types of rock particles under different conditions. The specific steps of the experiment were as follows: (1) Crush the rock using a core crusher to obtain rock particles. (2) Collect 1 kg of rock powder with a particle size of 0.149 mm using a vibrating sieve and store it in a wide-mouth bottle for later use. (3) Weigh 50.0 g of the prepared core particles and place them into a high-temperature vessel containing 350 mL of fluid. (4) Place the high-temperature vessel with the rock particles into a roller furnace and roll it at a formation temperature of 80 °C for 24 h. (5) Remove the high-temperature vessel and allow it to cool to room temperature. The liquid and rock samples inside the vessel were poured onto a sample sieve with a mesh size of 0.42 mm and rinsed in a basin of distilled water for 1 min. The remaining rock particles were then placed in a constant temperature drying oven for 4 h. After cooling, they were left to stand in air for 24 h before weighing, with the final weight recorded as *m*. The formula for calculating the thermal rolling recovery rate is $m/50 \times 100\%$. Figure 11 illustrates the variation of thermal rolling recovery rates for the different core samples at various concentrations of the inhibitor (modified natural polymer IND30). As shown in Figure 11, rocks 3 and 12, which had a relatively low illite/smectite interlayer content, exhibited generally high thermal rolling recovery rates (over 96%), indicating a weak overall hydration–dispersion capacity. Conversely, rocks 4 and 10, which had a high illite/smectite interlayer content, demonstrated thermal rolling recovery rates below 85%, indicating severe hydration–dispersion and a significant loss of rock particles during the thermal rolling process. However, with the addition of field

inhibitors, the hydration–dispersion capacity of rocks 4 and 10 could be effectively reduced, leading to improved thermal rolling recovery rates. When the inhibitor concentration was 0.25%, the thermal rolling recovery rates for rocks 4 and 10 could be increased to over 94%.

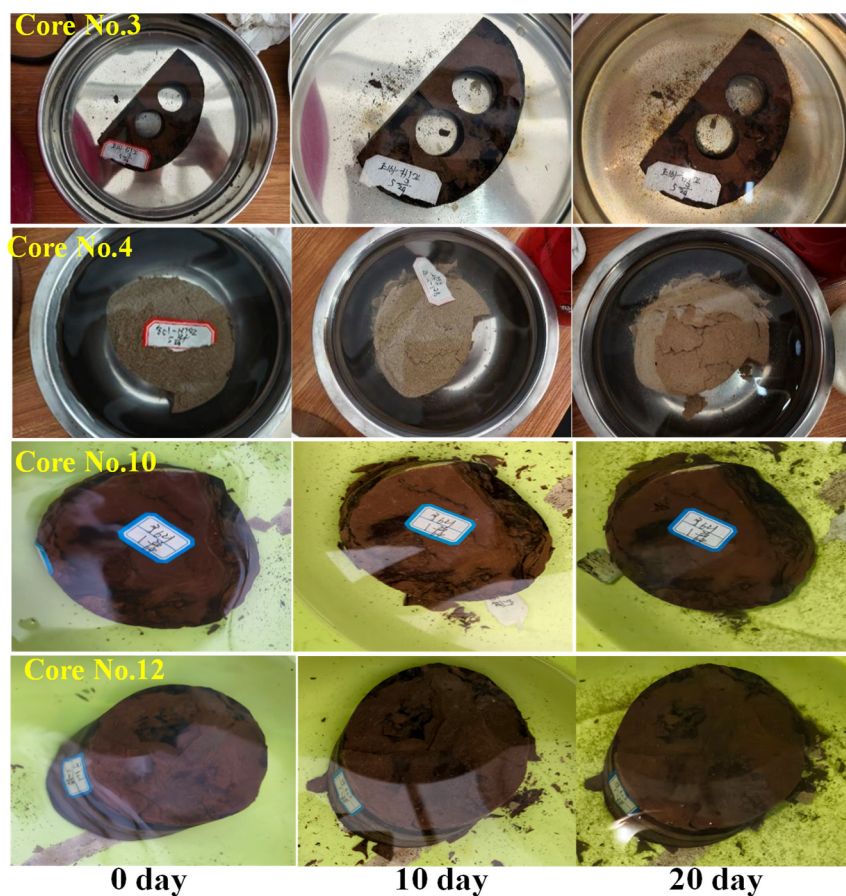


Figure 9. Hydration and dispersion behavior of reservoir rocks in loss zones at different soaking times.



Figure 10. Comparison of main and side views of core 10 before and after soaking in distilled water.

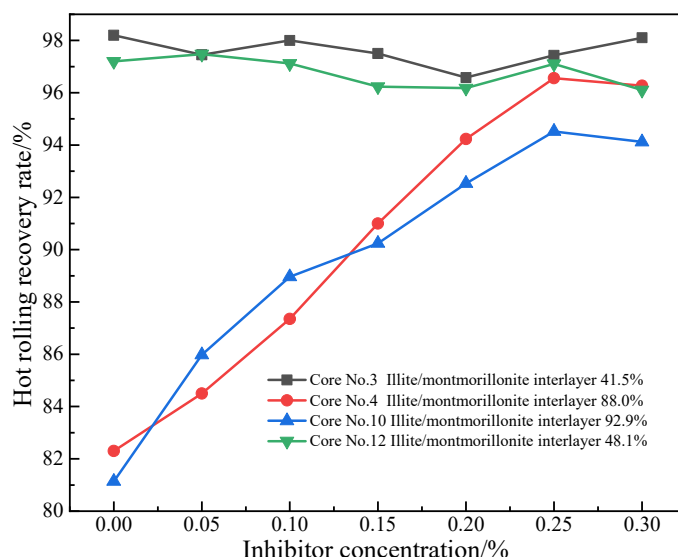


Figure 11. Variation of thermal rolling recovery rates of leakage layer rocks under different inhibitor concentrations.

4. Analysis of the Mechanical Properties of Rocks Surrounding the Wellbore

The content of Sections 1 and 2 has confirmed that the drilling loss in the Zhengning oilfield is related to natural fractures and the hydration–dispersion of the rocks. During the drilling process, the mechanical properties of the rocks surrounding the wellbore directly influence the loss pressure and the propagation of natural fractures. Based on this, we conducted true triaxial compression experiments on core samples from the same leakage layer to study the impact of natural fractures on the mechanical properties of leakage layer rocks. The experimental procedure was as follows: (1) Obtain standard cylindrical rock samples using a wire-cutting mechanism. (2) After polishing the surface of the rock samples, place them in the sample-holding device. (3) Apply confining pressure to the sample based on the in situ stress values obtained from well logging interpretation data. (4) Apply axial pressure and monitor the stress–strain changes of the sample.

As shown in Figure 12, after the triaxial compression experiments, the crack propagation in core samples 2 and 8 is illustrated, with red lines representing existing natural fractures and blue lines indicating fractures generated during the compression tests. Figure 13 presents the stress–strain curves obtained from these experiments. From Figure 12, it is evident that under identical pore-throat structures and mineral compositions, natural fractures significantly affected the mechanical properties of the leakage layer rocks. Cores without natural fractures primarily exhibited longitudinal fractures after triaxial compression, with a simple morphology and fewer occurrences. In contrast, cores with natural fractures exhibited complex fracture patterns, generating shear fractures that communicate with the natural fractures, leading to a substantial increase in the number of fractures upon failure. Combining insights from Figure 13, it is clear that the presence of natural fractures considerably reduced the compressive strength of the rocks under the same pore-throat structure and mineral composition. The rocks without natural fractures showed a steep stress–strain curve, indicating dense, hard rocks with strong elastic properties. Conversely, for the rocks with natural fractures, the curve was more gradual, suggesting higher Poisson’s ratios and greater plasticity. Furthermore, considering the clay mineral content analysis from Section 1, the rocks with a higher kaolinite content (core sample 8) exhibited greater compressive strength compared with those with a lower kaolinite content (core sample 2). Overall, this

analysis indicates that the presence of natural fractures in leakage layer rocks significantly decreases their strength and increases the risk of wellbore collapse and failure.

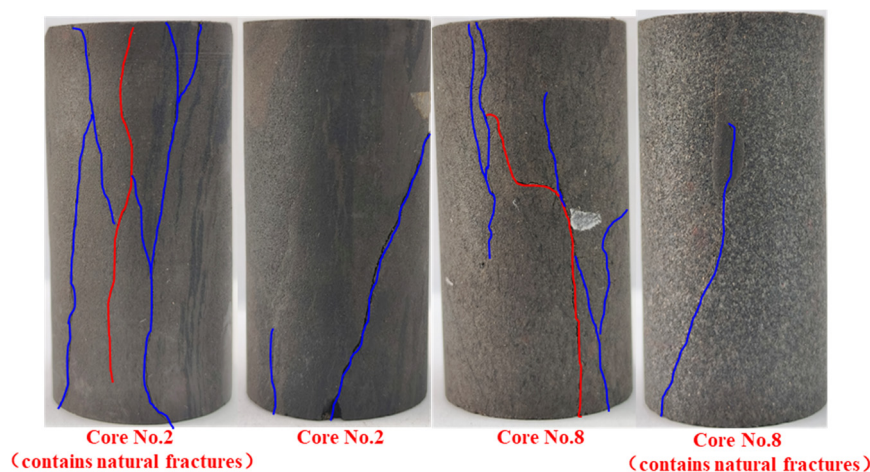


Figure 12. Results of true triaxial compression experiments for leakage layer core samples 2 and 8 (red lines represent natural fractures, while blue lines represent cracks generated during the mechanical experiments).

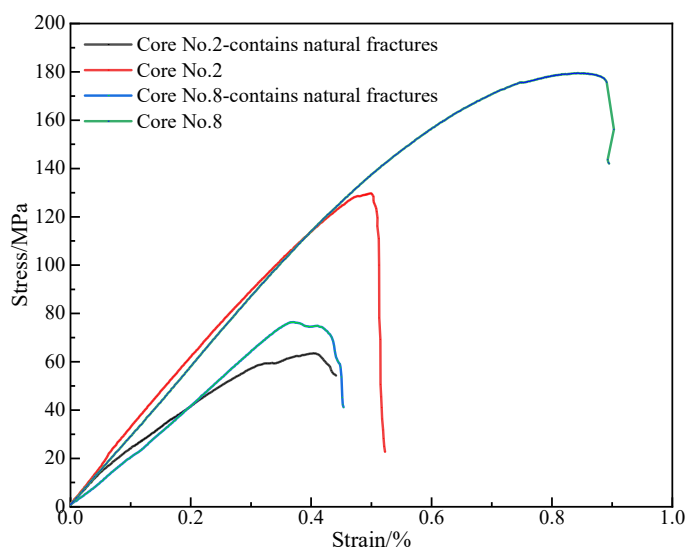


Figure 13. Stress–strain curves from true triaxial compression experiments for leakage layer core samples 2 and 8.

During the drilling process, the immersion of drilling fluid may cause hydration–dispersion in rocks, affecting their mechanical properties. In the previous two sections, we confirmed that when the relative content of illite/smectite interlayers exceeds 80% in clay minerals, the hydration–dispersion of the rocks becomes severe. For this section, we conducted a comparative analysis of the effects of drilling fluid immersion on the mechanical properties of core samples 4 and 8, selecting rocks without natural fractures for true triaxial mechanical experiments to eliminate the influence of natural fractures on the laboratory results. Figure 14 presents the results of the true triaxial compression experiments for leakage layer core samples 4 and 8, with the corresponding stress–strain curves shown in Figure 15. From Figure 14, it can be observed that in rocks that were not immersed in drilling fluid, the fracture morphology after failure was relatively simple, with fewer fractures. However, after immersion in drilling fluid, the fracture patterns became significantly more complex, with numerous branching fractures surrounding the main fracture, resulting in a substantial increase in the number of fractures. Figure 15 illustrates that under

the same pore-throat structure and mineral composition, the compressive strength of the rocks decreased by over 25% following immersion in drilling fluid, indicating a significant impact of hydration–dispersion on the mechanical properties of the rocks. The stress–strain curve for rocks not immersed in drilling fluid was steep, indicating dense and hard rocks with a low Poisson’s ratio. In contrast, after immersion in drilling fluid, the stress–strain curve shifted to the right, becoming more gradual, suggesting that hydration–dispersion increased the plasticity of the rocks and raised the Poisson’s ratio. In summary, it can be concluded that during the drilling process in the Zhengning oilfield, the immersion of drilling fluid may be one of the reasons for the reduction in rock strength and the occurrence of wellbore loss incidents. For layers with a high content of illite/smectite interlayers, it is essential to add inhibitors during drilling to prevent the hydration–dispersion of the rocks.

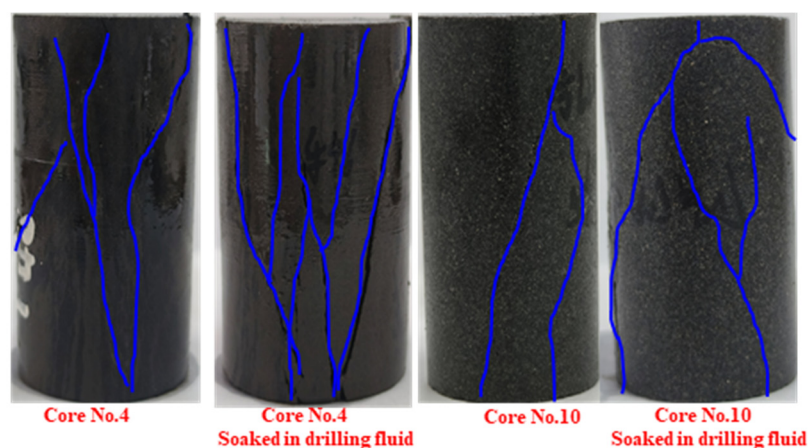


Figure 14. Results of true triaxial compression experiments for leakage layer core samples 4 and 8 (blue lines represent cracks generated during the mechanical experiments, with an immersion time of 48 h).

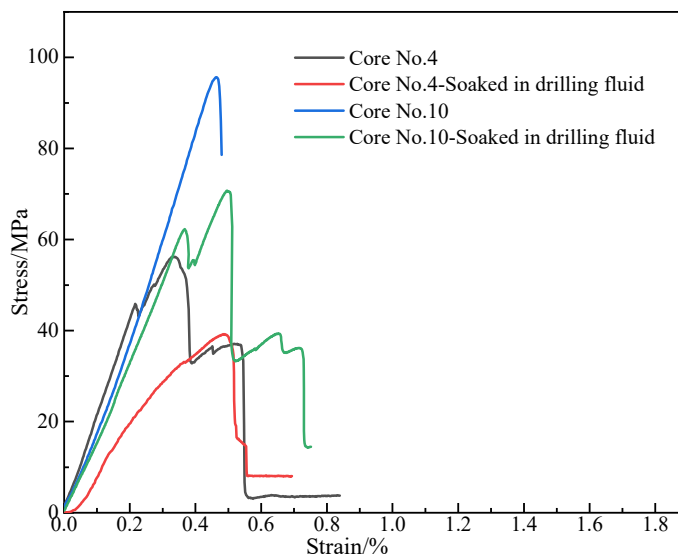


Figure 15. Stress–strain curves from true triaxial compression experiments for leakage layer core samples 4 and 10.

5. Conclusions

This study, based on core drilling from the Zhengning oilfield in the Ordos Basin, conducted laboratory experiments to investigate the mechanisms behind drilling loss incidents in the region. The main findings are as follows:

- (1) The average porosity of the leakage layer reservoir rocks is 3.89%, with an average permeability of 0.044 mD. The clay mineral content exceeds 40%, generally high in the rocks.
- (2) The leakage layer reservoir rocks are widely distributed with natural fractures. The macro natural fractures are most prevalent in the 0.2 mm to 0.3 mm range, accounting for over 30%, while micro natural fractures are primarily between 0.5 μm and 2 μm .
- (3) When the relative content of illite/smectite interstratification in clay minerals exceeds 80%, the rock absorbs water rapidly, exhibits strong hydration–dispersion behavior, and presents a thermal recovery rate of less than 85%. After immersion in distilled water, the rock tends to flake off in chunks and the fracture width of the horizontal stratification fractures significantly increases, forming distinct longitudinal fractures.
- (4) The presence of natural fractures significantly weakens the strength of the leakage layer rocks, causing them to exhibit plastic behavior. The strong hydration–dispersion destabilizes the rock structure, facilitating fracture interconnection and further reducing rock strength.
- (5) During drilling, natural fractures provide pathways for drilling fluid loss. The macro natural fractures extend under borehole pressure, interconnecting with micro fractures and ultimately leading to increased fluid loss due to the hydration–dispersion effects.
- (6) To improve drilling safety in the Zhengning oilfield, it is recommended to enhance the drilling fluid’s sealing capacity for natural fractures of different fracture width levels and to strengthen the suppression effect of the drilling fluid on rock hydration–dispersion.

Author Contributions: Conceptualization, T.G. and S.Y.; methodology, Y.X.; software, L.Z.; validation, F.P. and X.S.; formal analysis, T.F.; investigation, H.W.; resources, D.Z.; data curation, Y.X.; writing—original draft preparation, L.Z.; writing—review and editing, X.S.; visualization, F.P.; supervision, T.F.; project administration, H.W.; funding acquisition, D.Z. All authors have read and agreed to the published version of the manuscript.

Funding: This research was funded by the National Natural Science Foundation of China, grant number U23B2089, and the Shaanxi Provincial Natural Science Basic Research Program Project, grant number 2024JC-YBQN-0554.

Data Availability Statement: The data presented in this study are available upon request from the corresponding author: 24111010032@stumail.xsyu.edu.cn.

Conflicts of Interest: Authors Tuan Gu, Shugang Yang, Yunfeng Xiao, Linpeng Zhang and Tao Fan are employed by Exploration and Development Research Institute of Liaohe Oilfield Company, PetroChina. The paper reflects the views of the scientists and not the company.

References

1. Yang, H.; Fu, J.H.; Wei, X.S.; Liu, X.S. Sulige field in the Ordos Basin: Geological setting, field discovery and tight gas reservoirs. *Mar. Pet. Geol.* **2008**, *25*, 387–400. [[CrossRef](#)]
2. Yao, J.L.; Deng, X.Q.; Zhao, Y.D.; Han, T.Y.; Chu, M.J.; Pang, J.L. Characteristics of tight oil in Triassic Yanchang Formation, Ordos Basin. *Pet. Explor. Dev.* **2013**, *40*, 161–169. [[CrossRef](#)]
3. Wang, H.; Zhou, D.; Zou, Y.; Zheng, P. Effect mechanism of seepage force on the hydraulic fracture propagation. *Int. J. Coal Sci. Technol.* **2024**, *11*, 43. [[CrossRef](#)]
4. Xu, C.; Kang, Y.; Chen, F.; You, Z. Fracture plugging optimization for drill-in fluid loss control and formation damage prevention in fractured tight reservoir. *J. Nat. Gas Sci. Eng.* **2016**, *35*, 1216–1227. [[CrossRef](#)]
5. Zhu, J.; You, L.; Li, J.; Kang, Y.; Zhang, J.; Zhang, D.; Huang, C. Damage evaluation on oil-based drill-in fluids for ultra-deep fractured tight sandstone gas reservoirs. *Nat. Gas Ind. B* **2017**, *4*, 249–255. [[CrossRef](#)]
6. Aljubran, M.; Ramasamy, J.; Albassam, M.; Magana-Mora, A. Deep Learning and Time-Series Analysis for the Early Detection of Lost Circulation Incidents During Drilling Operations. *IEEE Access* **2021**, *9*, 76833–76846. [[CrossRef](#)]
7. Lavrov, A. *Lost Circulation: Mechanisms and Solutions*; Gulf Professional Publishing: Oxford, UK, 2016.

8. Feng, F.; Gray, K.E. Modeling Lost Circulation Through Drilling-Induced Fractures. *SPE J.* **2018**, *23*, 205–223. [[CrossRef](#)]
9. Fuh, G.-F.; Morita, N.; Boyd, P.A.; McGoffin, S.J. A New Approach to Preventing Lost Circulation While Drilling. In Proceedings of the SPE Annual Technical Conference and Exhibition, Washington, DC, USA, 4–7 October 1992.
10. Howard, G.C.; Scott, P.P. An analysis and the control of lost circulation. *Trans. Am. Inst. Min. Metall. Eng.* **1951**, *192*, 171–182. [[CrossRef](#)]
11. Wang, H.; Zhou, D. Mechanistic study on the effect of seepage force on hydraulic fracture initiation. *Fatigue Fract. Eng. Mater. Struct.* **2024**, *47*, 1602–1619. [[CrossRef](#)]
12. Li, S.; Purdy, C. Maximum Horizontal Stress and Wellbore Stability While Drilling: Modeling and Case Study. In Proceedings of the SPE Latin American and Caribbean Petroleum Engineering Conference, Lima, Peru, 1–3 December 2010.
13. Ukaeru, F.C.; Igwilo, K.; Chikwe, A.; Ubanozie, O. Impact of Near-Wellbore Stress in Wellbore Integrity Analysis: Wellbore Fracture Strengthening Approach. *Eur. J. Sci. Innov. Technol.* **2024**, *4*, 187–206.
14. Jia, L.; Chen, M.; Hou, B.; Sun, Z.; Jin, Y. Drilling fluid loss model and loss dynamic behavior in fractured formations. *Pet. Explor. Dev. Online* **2014**, *41*, 105–112. [[CrossRef](#)]
15. Majidi, R.; Miska, S.Z.; Ahmed, R.; Yu, M.; Thompson, L.G. Radial flow of yield-power-law fluids: Numerical analysis, experimental study and the application for drilling fluid losses in fractured formations. *J. Pet. Sci. Eng.* **2010**, *70*, 334–343. [[CrossRef](#)]
16. Yang, J.; Sun, J.; Bai, Y.; Lv, K.; Zhang, G.; Li, Y. Status and Prospect of Drilling Fluid Loss and Lost Circulation Control Technology in Fractured Formation. *Gels* **2022**, *8*, 260. [[CrossRef](#)] [[PubMed](#)]
17. Zhiyu, W.; Changming, H.; Liang, L.; Chao, Y.; Hui, L. Theoretical Analysis of Drilling Fluid Flow for Maxi-Horizontal Directional Drilling. *J. Pipeline Syst. Eng. Pract.* **2024**, *15*, 04024050. [[CrossRef](#)]
18. Gazaniol, D.; Forsans, T.; Boisson, M.J.F.; Piau, J.-M. Wellbore Failure Mechanisms in Shales: Prediction and Prevention. *J. Pet. Technol.* **1995**, *47*, 589–595. [[CrossRef](#)]
19. Wang, B.; Sun, J.; Shen, F.; Li, W.; Zhang, W. Mechanism of wellbore instability in continental shale gas horizontal sections and its water-based drilling fluid countermeasures. *Nat. Gas Ind. B* **2020**, *7*, 680–688. [[CrossRef](#)]
20. Zhao, X.; Qiu, Z.; Wang, M.; Xu, J.; Huang, W. Experimental investigation of the effect of drilling fluid on wellbore stability in shallow unconsolidated formations in deep water. *J. Pet. Sci. Eng.* **2019**, *175*, 595–603. [[CrossRef](#)]
21. Ma, J.; Pang, S.; Zhang, Z.; Xia, B.; An, Y. Experimental Study on the Polymer/Graphene Oxide Composite as a Fluid Loss Agent for Water-Based Drilling Fluids. *ACS Omega* **2021**, *6*, 9750–9763. [[CrossRef](#)] [[PubMed](#)]
22. Nasser, J.; Jesil, A.; Mohiuddin, T.; Ruqeshi, M.A.; Devi, G.; Mohataram, S. Experimental Investigation of Drilling Fluid Performance as Nanoparticles. *World J. Nano Sci. Eng.* **2013**, *3*, 5. [[CrossRef](#)]
23. Al-Hameedi, A.T.T.; Alkinani, H.H.; Dunn-Norman, S.; Al-Alwani, M.A.; Alshammari, A.F.; Alkhamis, M.M.; Mutar, R.A.; Al-Bazzaz, W.H. Experimental investigation of environmentally friendly drilling fluid additives (mandarin peels powder) to substitute the conventional chemicals used in water-based drilling fluid. *J. Pet. Explor. Prod. Technol.* **2020**, *10*, 407–417. [[CrossRef](#)]
24. Ezeakacha, C.P.; Salehi, S. Experimental and statistical investigation of drilling fluid loss in porous media: Part 2 (Fractures). *J. Nat. Gas Sci. Eng.* **2019**, *65*, 257–266. [[CrossRef](#)]
25. Srivatsa, J.T.; Ziaja, M.B. An Experimental Investigation on Use of Nanoparticles as Fluid Loss Additives in a Surfactant—Polymer Based Drilling Fluids. In Proceedings of the International Petroleum Technology Conference, Bangkok, Thailand, 15–17 November 2011.
26. Kong, C.; Sun, Y.; Li, C.; Zhao, J.; Zhu, X. Numerical simulation study on impact factors to dynamic filtration loss. *J. Pet. Explor. Prod. Technol.* **2024**, *14*, 593–607. [[CrossRef](#)]
27. Yang, L.; Cheng, Z.G. Numerical Simulation of Large-Diameter Annular Pressure Loss in Riser Segment of Deep-Water Drilling. *Adv. Mater. Res.* **2013**, *868*, 510–516. [[CrossRef](#)]
28. Xu, C.; Liu, L.; Yang, Y.; Kang, Y.; You, Z. An innovative fracture plugging evaluation method for drill-in fluid loss control and formation damage prevention in deep fractured tight reservoirs. *Fuel* **2024**, *358*, 130123. [[CrossRef](#)]
29. ALi, A.; Gao, S.; Zhang, G.; Zeng, Y.; Hu, Y.; Zhai, R.; Dong, A.; Zhang, J. A Review in Polymers for Fluid Loss Control in Drilling Operations. *Macromol. Chem. Phys.* **2024**, *225*, 2300390. [[CrossRef](#)]
30. Sun, J.; Yang, J.; Bai, Y.; Lyu, K.; Liu, F. Research progress and development of deep and ultra-deep drilling fluid technology. *Pet. Explor. Dev. Online* **2024**, *51*, 1022–1034. [[CrossRef](#)]
31. Wu, S.; Li, L.; Li, X.; Yue, Z.Q. Characterizing strength and location of continental oil shale with drilling process monitoring in Southern Ordos Basin, China. *J. Rock Mech. Geotech. Eng.* **2024**. [[CrossRef](#)]
32. Liu, J.; Zhang, G.; Bai, J.; Ding, W.; Yang, H.; Liu, Y. Quantitative prediction of the drilling azimuth of horizontal wells in fractured tight sandstone based on reservoir geomechanics in the Ordos Basin, central China. *Mar. Pet. Geol.* **2022**, *136*, 105439. [[CrossRef](#)]

33. Zhang, X.; Dang, B.; Wang, X.; Luo, S.; Chen, B.; Zheng, L. Acid-Soluble Drilling Fluid in the Northern Carbonate Reservoir of the Yishan Slope in the Ordos Basin. *Energies* **2023**, *16*, 6020. [[CrossRef](#)]
34. Zhang, X.; You, L.; Kang, Y.; Zhang, C.; Zhang, G.; Tan, Q. Formation damage control of saline-lacustrine fractured tight oil reservoir during well drilling. *Arab. J. Geosci.* **2020**, *13*, 1087. [[CrossRef](#)]

Disclaimer/Publisher's Note: The statements, opinions and data contained in all publications are solely those of the individual author(s) and contributor(s) and not of MDPI and/or the editor(s). MDPI and/or the editor(s) disclaim responsibility for any injury to people or property resulting from any ideas, methods, instructions or products referred to in the content.